Resolution of 3D elongated deep conductive bodies embedded in a 2D background conductivity structure by 3D and 2D magnetotelluric inversion

Kristina Tietze[1,2], Oliver Ritter[1,2]

1 Helmholtz Centre Potsdam - German Research Centre For Geosciences GFZ, Department 2, Section 2.2, Telegrafenberg, 14473 Potsdam

2 Free University Berlin, Department of Earth Sciences, Malteserstr. 74-100, 12249 Berlin

Contact: kristina.tietze@gfz-potsdam.de

Summary

In recent years, 3D inversion has become a practical, if still computationally demanding, tool for interpreting MT data. This interpretation approach appears to hold great promise by overcoming the simplifications necessary to force the 3D nature of the real world into 2D models and thus producing more realistic and truthful images of the subsurface. In a series of geologic situations, however, we can identify a 2D regional structure in which local 3D structures are embedded. Based on synthetic data, we explore the resolution of an elongated highly conductive zone (HCZ) with varying along-strike extents embedded in a 2D regional resistivity structure with 3D and 2D inversion algorithms.

Our results show that both inversion approaches recover the HCZ for large along-strike extents; for shorter extents, surprisingly 2D inversion better recovered the subsurface structures. In presence of high conductivity contrasts and wide conductivity contrasts 3D inversion can fail to resolve structures of predominantly 2D character. In 2D inversion, the weak 3D nature of the ocean included in the synthetic model impaired the impedance-only inversion results for short HCZ extent and problems occurred if phase values below 5° were present in the data set.

Introduction

With advancing computational resources, three-dimensional (3D) inversion techniques have become practical in recent years and are now a more widely used tool for magnetotelluric (MT) data interpretation. A number of 3D inversion programs using various approaches for both forward modelling and inversion have been developed (e.g. Mackie *et al.* 2001; Siripunvaraporn *et al.* 2005a; Egbert & Kelbert 2012). Several studies applying 3D inversion algorithms to synthetic and field data show clear advantages over a 2D data interpretation as no restrictions on the dimensionality of the subsurface structure apply (e.g. Newman *et al.* 2003; Patro & Egbert 2011; Siripunvaraporn *et al.* 2005b). If data contains 3D structures, 2D interpretation of the data set can result in misleading subsurface models. Ledo (2005) outlined the dangers of 2D inversion of 3D structures depending on the orientation of the 3D structure relative to a 2D background structure.

3D and 2D inversion of a real-world data set from the San Andreas fault (SAF) in central California revealed a pronounced zone of high conductivities (HCZ) at depths of 15 – 30 km which extends parallel to a regional 2D background resistivity structure (Becken *et al.* 2008b, 2011; Tietze & Ritter *subm.*). Differences between 3D and 2D results are related to conductance, location, and shape of the HCZ. We used a 3D synthetic test model comprising the dominant structures of the survey area to investigate various aspects of 3D and 2D inversion related to the specific subsurface structure. Here, we focus on the impact of a varying finite along-strike extent of the HCZ on the outcome of 3D and 2D inversion.

3D and 2D forward modelling

The SYNPRK model (Fig. 1) comprises dominant structures of the survey area near Parkfield as revealed by 2D and 3D inversion: A highly conductive (1 Ωm) 20 km wide and 25 km high zone (HCZ) with its top at 17 km depth is embedded in a background structure mimicking a highly resistive Pacific Plate (2000 Ωm) and an intermediately resistive American Plate (200 Ωm). The elongated HCZ is located approximately 30 km southwest of the surface trace of the SAF. The top layers of the model comprise sedimentary material (3 Ωm) of varying thickness (2.2 km, 6.8 km). The Pacific Ocean (0.3 Ωm) is included according to bathymetry. The HCZ was modelled with along-strike extents of 258 km, 554 km, and 1150 km symmetric to the station array; the SYNPRK-h model variant lacks the HCZ. 3D synthetic data were calculated for a regular site layout with profile distances of 10 km, even site spacing of 10 km along the profiles and with 18 logarithmically distributed periods between 0.08 s and 11,000 s. 3 % Gaussian noise was added to the synthetic data prior to inversion. For 3D forward modelling we used ModEM3D (Egbert & Kelbert 2012) and WinGLink (Mackie *et al.* 1994).

In all modelling steps, the coordinate systems for model grid and data are identical. The *x*-axis is aligned with strike of the regional SYNPRK conductivity structure and *y* points parallel to the profiles (cf. Fig. 1). In this coordinate system, tangential-electric and tangential-magnetic modes

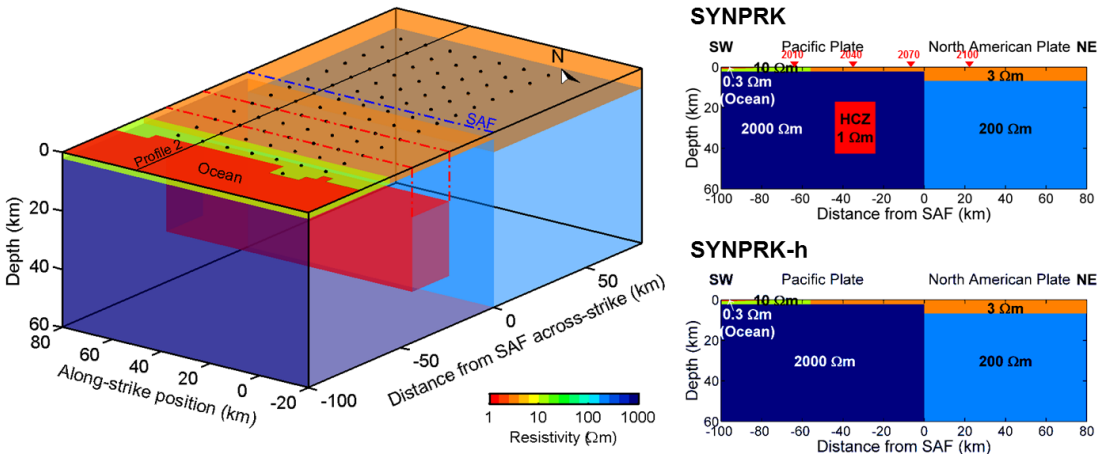

Figure 1: The SYNPRK resistivity model includes the main structural features revealed by 2D and 3D inversion of magnetotelluric data from the San Andreas fault near Parkfield, California. We investigated the impact of the along-strike extent of the HCZ. The highly conductive zone (HCZ) extends 268 - 1150 km along-strike; the Pacific Ocean is integrated according to true bathymetry. All other structures extend to the model edges. For the SYNPRK-h variant, the HCZ was removed.

of the 3D SYNPRK data set maximally separate. For the SYNPRK-h variant, Phase Tensor beta values (Caldwell *et al.* 2004) are small at all periods (Fig 2), which illustrates that the ocean constitutes only weak 3D effects (cf. Fig. 3). The 3D characteristic of the HCZ shows as elevated beta values at sites above the HCZ for periods between 100 s and 2000 s yielding maximum values at 181 s for an along-strike extent of 268 km and at 724 s for 1150 km (Fig. 2). As the data set is predominantly 2D we only consider components Zxy, Zyx, and Ty in the following.

Comparing FWD responses at selected sites, the impact of the HCZ can be identified for periods > 10 s (Fig. 4). The impact is limited to the Zxy and Ty components, which constitute the 2D TE

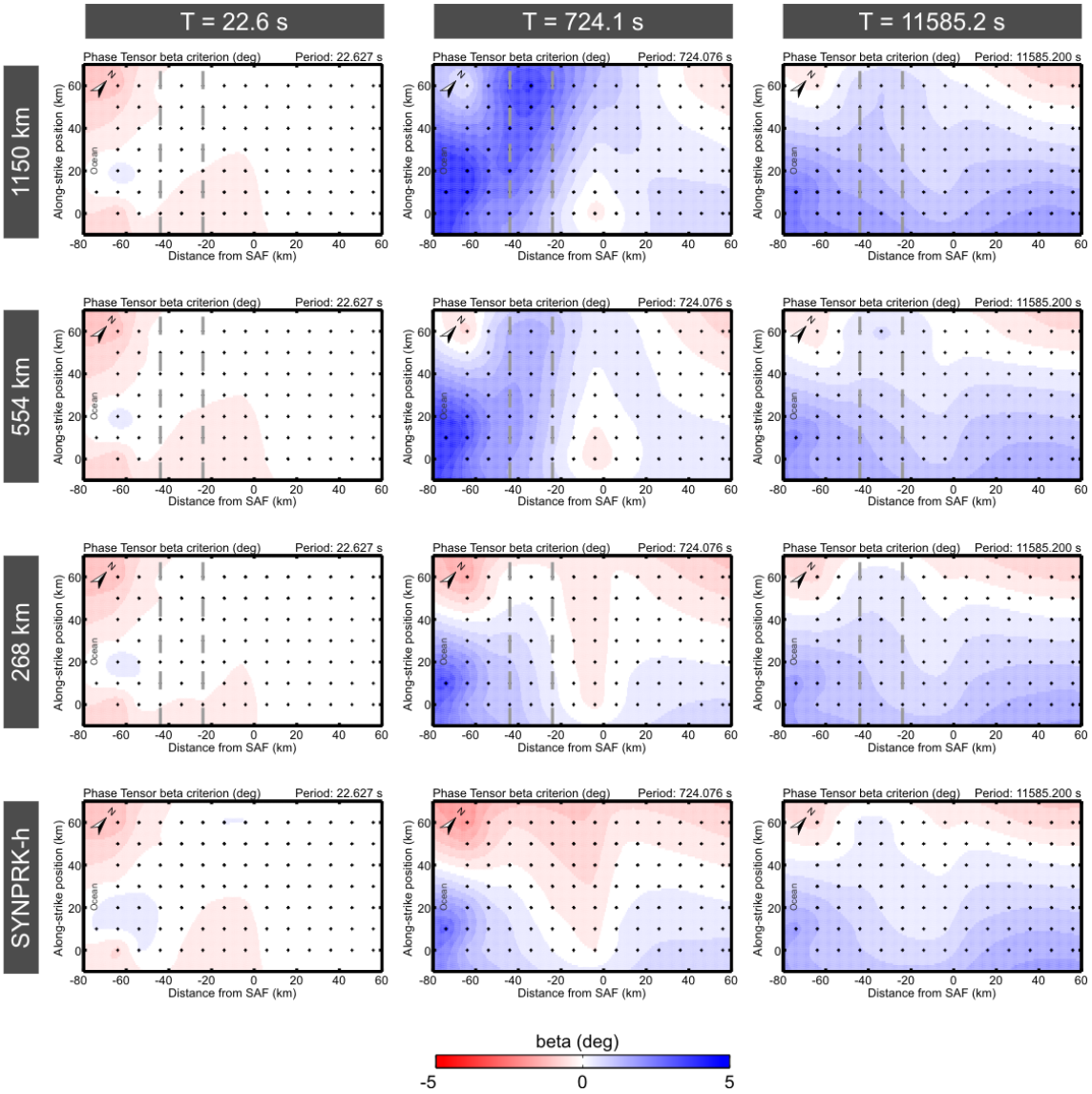

Figure 2: Phase tensor beta values for the SYNPRK model variants. Beta values significantly deviating from zero at intermediate periods (724 s) at sites above the HCZ illustrate the 3D characteristic of the HCZ. Consistently small beta values of the SYNPRK-h data (lowermost panel), illustrate the predominant 2D nature of the background structure.

mode. Zyx data are only marginally affected by the HCZ; the 3D Zyx-responses are not distinguishable in Fig. 4. For increasing along-strike extent of the HCZ, the 3D FWD responses for Zxy and Ty gradually change their shape towards a bound which resembles the response of an infinite, truly 2D HCZ. The Zxy and Ty responses for an infinite HCZ and a 2D ocean obtained with 2D FWD modelling (Rodi & Mackie 2001) along profile 2 (cf. Fig. 1) appear inconsistent with the 3D response behaviour at first sight. Also the yx-phase minima between 10 s and 1000 s are consistently weaker expressed in the 2D response. Comparing 3D FWD responses obtained with ModEM3D and WinGLink (Mackie et al. 1994) for the SYNPRK model we were able to exclude side effects from grid setup or other aspects of the 3D FWD calculation. In fact, the response differences originate from the 3D effect of the Pacific Ocean, which is mainly caused by the strike axis of the continental margin lying at an angle to the strike of the 2D SYNPRK structure (cf. Fig. 3). When modelling the 3D SYNPRK structures with a purely 2D ocean, where strike of bathymetry is parallel to the SYNPRK structures, 3D results are consistent with the 2D WinGLink result for an infinite HCZ (not shown).

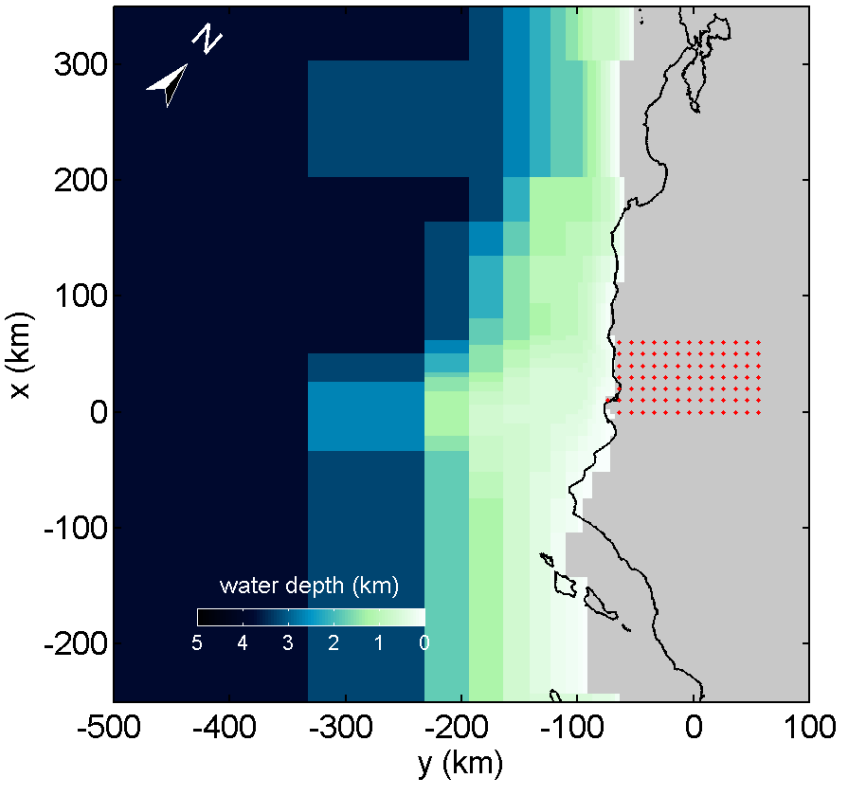

Figure 3: Bathymetry of the Pacific Ocean in the SYNPRK model. In the vicinity of the site array (red dots) the strike direction of the bathymetric fabric and the continental margin is oblique to the SYNPRK structure (aligned with model grid). Thus, the conductive sea water body has some 3D impact on the data.

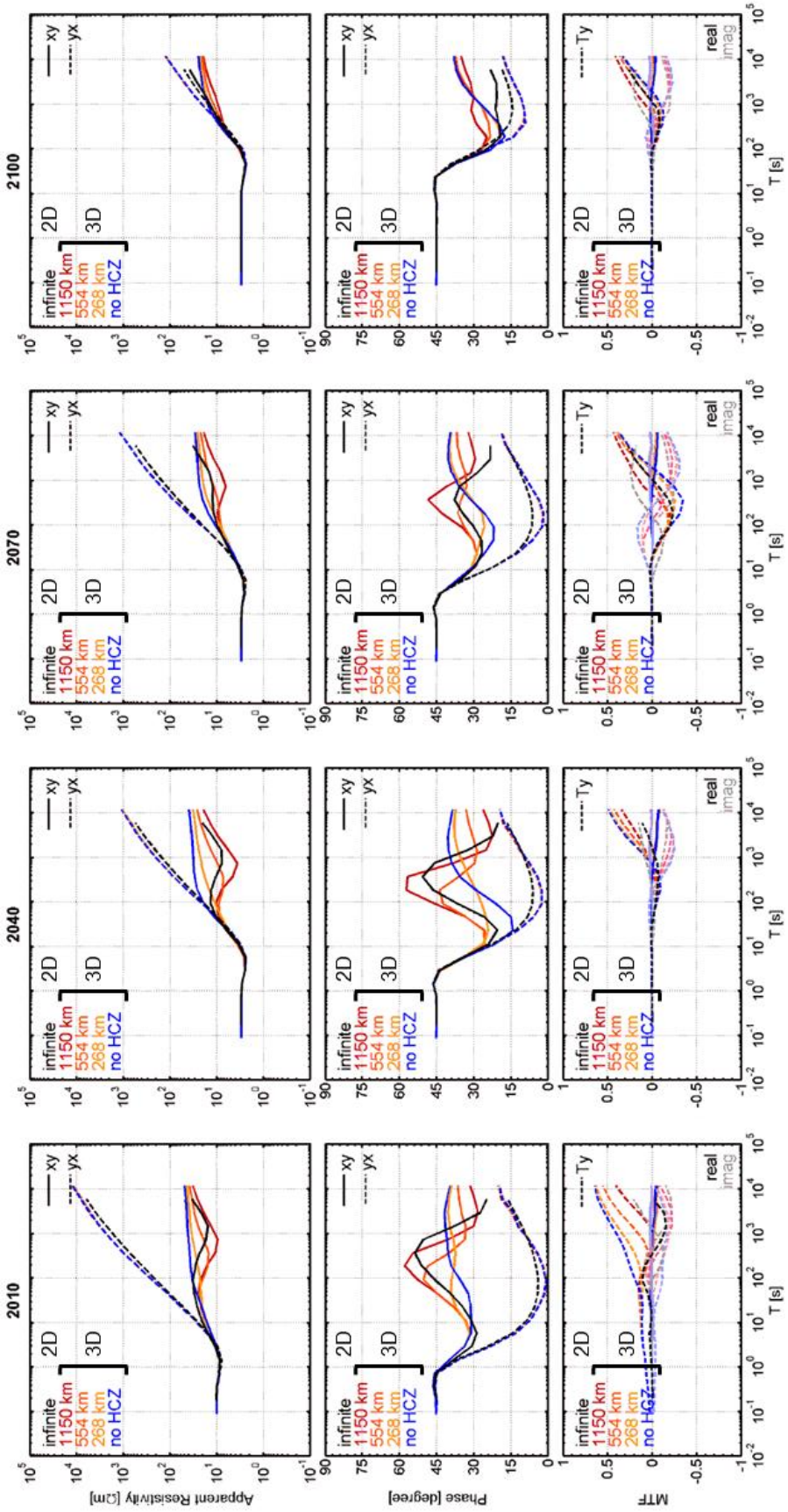

Figure 4: FWD responses along profile 2 for different along-strike extents of the HCZ, for site locations see Fig. 1. The impact of the HCZ manifests at periods > 10s at sites in the vicinity of the HCZ and periods > 100 s towards the inland end of the survey array and is limited to the Zxy and Ty components. For finite along-strike extents, ModEM3D response curves smoothly vary. The 2D WinGLink response for an infinite HCZ, however, does not fit into the pattern because of the 2D approximation of the 3D bathymetry.

3D and 2D inversion results

For 3D inversion (ModEM3D) we used off-diagonal impedances Zxy and Zyx, and/or the across-strike vertical magnetic transfer function (VTF) component (Ty) of all 92 array sites. Error floors are set to 3 % for impedances and 0.02 for Ty. The central model domain comprising the station array and the coastal area was horizontally discretized by a 4 km × 4 km mesh of 10 Ωm. A resistivity of 0.3 Ωm was assigned to the ocean cells and this model domain was kept fixed at all times during the inversion. Model covariances (regularization parameters) were set to 0.4, 0.2, and 0.3 for *x*-, *y*-, and *z*-directions, respectively, enforcing a higher regularization along-strike. Further details concerning the inversion parameters are described in the methods section in the appendix.

With 3D inversion the along-strike extent of the HCZ must exceed 500 km in order to be reliably revealed by both impedances and VTFs (Fig. 5). This is related to the inversion scheme of ModEM3D which penalizes deviations from a prior model. Thus, recovering the large range of conductivities of the SYNPRK model is a challenge, in particular, if homogeneous starting models are used. In all inversion models of the SYNPRK data set, a number of "additional" cells with high conductivity attached to the ocean can be observed. Obviously, the inversion tries to construct the desired resistivity contrast between coast and the seafloor. In terms of finding a minimal model norm, it is less costly to change some of the more conductive cells than a much larger volume of resistive cells, which would be necessary to recover the high-resistive Pacific Plate of the SYNPRK model extending beneath the ocean. However, the full intensity of the resistivity contrast is not reproduced; overall misfits close to the theoretical target of 1.0 cannot be achieved for inversion of SYNPRK impedance data which are sensitive to the absolute resistivity level. For the shortest along-strike extent, the impact of the HCZ is too low compared to the misfit due to the insufficient reproduction of the conductivity contrast along the coast.

For impedance-only inversion, the resistivity level beneath the station array and the top of the HCZ are well resolved. The location of the HCZ is shifted slightly inland with respect to the original position, as the artificial coastal conductor simulates some of the signature of the HCZ in the impedance data. In contrast, Ty-only inversion successfully recovers the lateral boundaries of the HCZ, as VTFs are particularly sensitive to horizontal conductivity changes. Due to the very low resistivities of the starting model, the HCZ is located at too shallow depth. When using higher resistivity values for the starting model, the HCZ is not resolved. Inverting for impedances and VTFs jointly, 3D inversion makes use of the strengths of either data type and well recovers both the location of the HCZ and the surrounding resistivity structure.

With 2D inversion using the algorithm of Rodi & Mackie (2001) recovering blocks with even shorter lateral extensions is successful (Fig. 6). We used standard inversion parameters (see methods section) and error floors of 10% for resistivities, 2% (0.6°) for phases, and 0.02 for Ty. Analogue to 3D modelling, bathymetry along profile 2 was integrated into the starting model and kept fixed (τ = 10,000) during inversion. Starting resistivities were 200 Ωm for Ty-only inversion and 50 Ωm for apparent resistivity/phase and joint inversions.

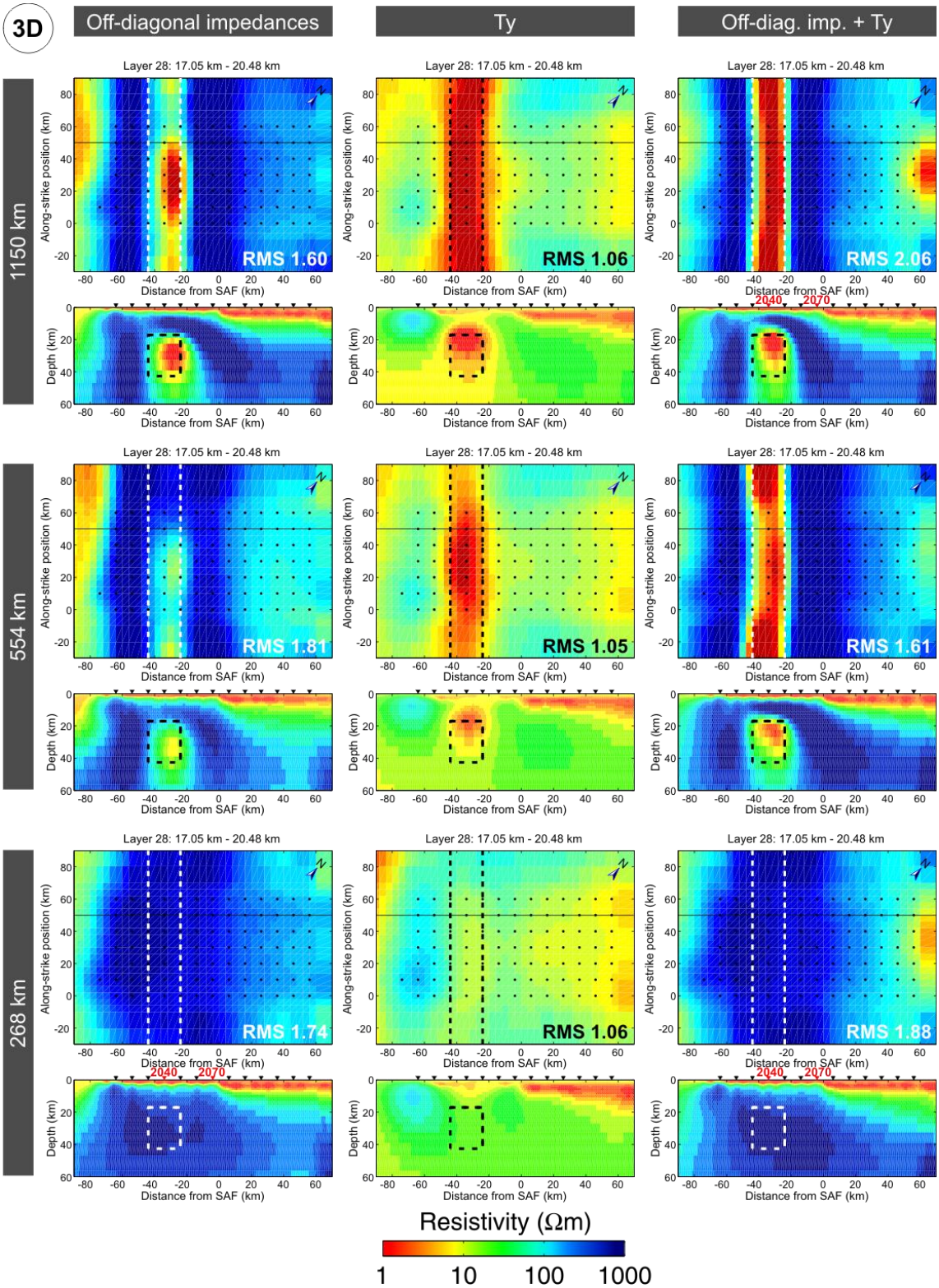

Figure 5: 3D inversion results as horizontal slices at the top of the HCZ (17 km) and along profile 2 (cf. Fig. 1). For 3D inversion the along-strike extent of the HCZ (dashed outline) must exceed 500 km to be recovered with some certainty. Insufficient recovery of the high conductivity contrast along the coastline and beneath the ocean, expressed in high final overall RMS values, inhibits resolving shorter HCZ versions.

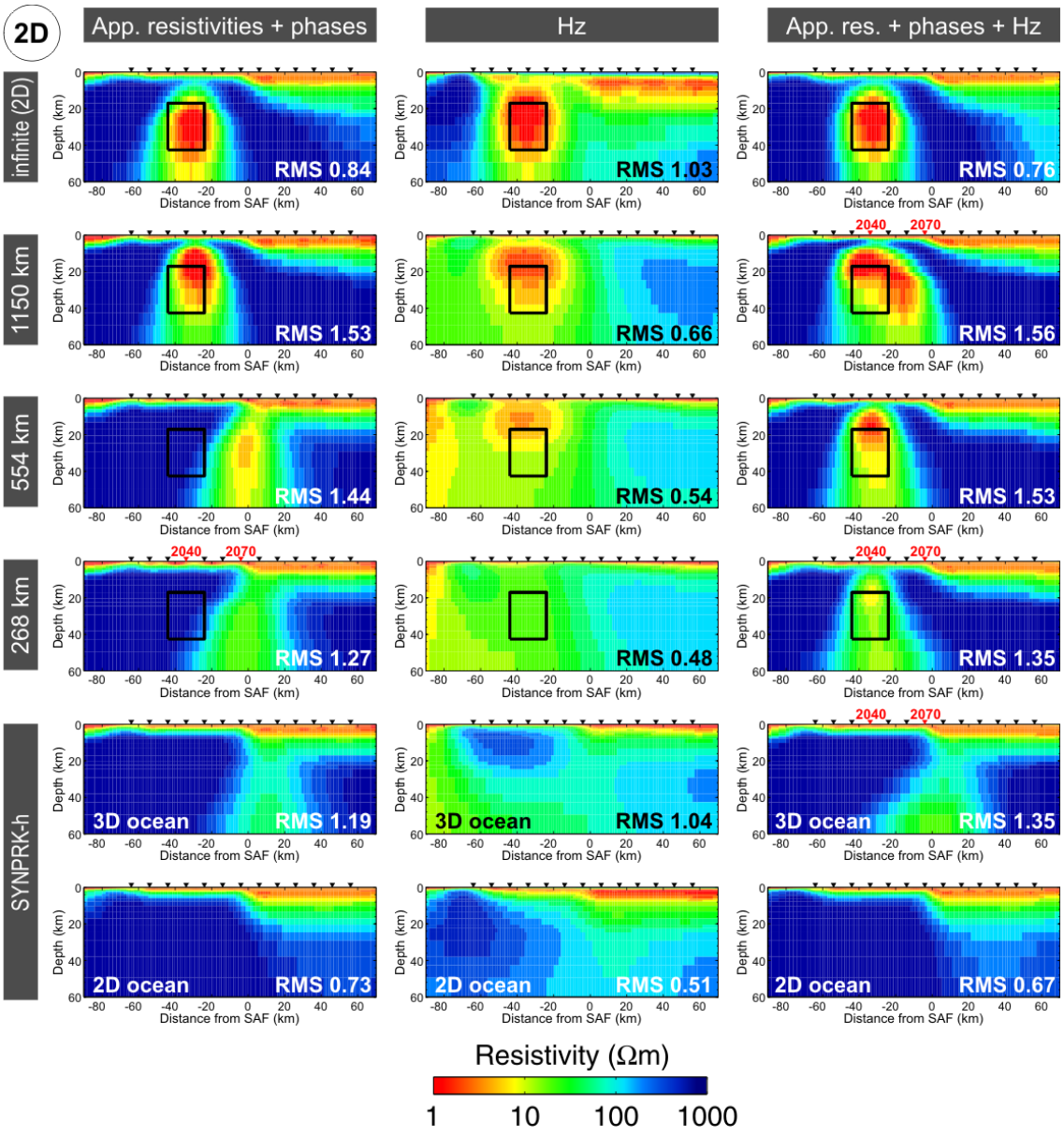

Figure 6: 2D inversion along profile 2 (cf. Fig 1) can recover the HCZ for all along-strike extents. Reliable images of the SYNPRK structure are, however, only achieved for joint inversion of apparent resistivities, phases, and VTFs. The shift of the HCZ towards the SAF and the blurred conductive region imaged beneath the SAF for the SYNPRK-h variant are related to the 3D characteristic of the bathymetry. In general, the HCZ is imaged at too shallower depth, if 3D modelling responses were inverted. Responses from sites marked in red are shown in Fig. 7.

Using only apparent resistivities (left column in Fig 6), the location of the HCZ is only well recovered for the variant with the longest extension. For shorter along-strike extents, the HCZ is shifted towards the SAF. Also for the SYNPRK-h variant which lacks the HCZ, 2D inversion images an artificial conductive region beneath the SAF. FWD modelling tests showed hardly any difference to completely homogeneous highly resistive deeper structures. This unexpected result is related to the 3D characteristic of the Pacific ocean (cf. Fig 4). Inverting the SYNPRK-h response comprising a 2D ocean, the continuous high resistivities of the deep subsurface are imaged correctly (lowermost panel in Fig 6). Ty-only inversion of the SYNPRK data, reliably

reveals the HCZ and its lateral position. The varying along-strike extent of the HCZ only affects the Ty-amplitude, which is largest for a HCZ length of 1150 km. However, even for the shortest along-strike extent considered here, the induction vectors still point nearly parallel to the profiles, the finite extent of the HCZ does not yet influence the VTFs. Thus, the behaviour of the profile-parallel Ty component is still consistent with an infinite 2D HCZ of decreased conductance. Hence, the image of the HCZ becomes weaker with shorter HCZ extent. Joint inversion of apparent resistivities, phases, and Ty successfully recovers the HCZ even for 258 km along-strike extent. All 2D inversion results of data comprising a 3D ocean, however, image the HCZ at too shallow depths.

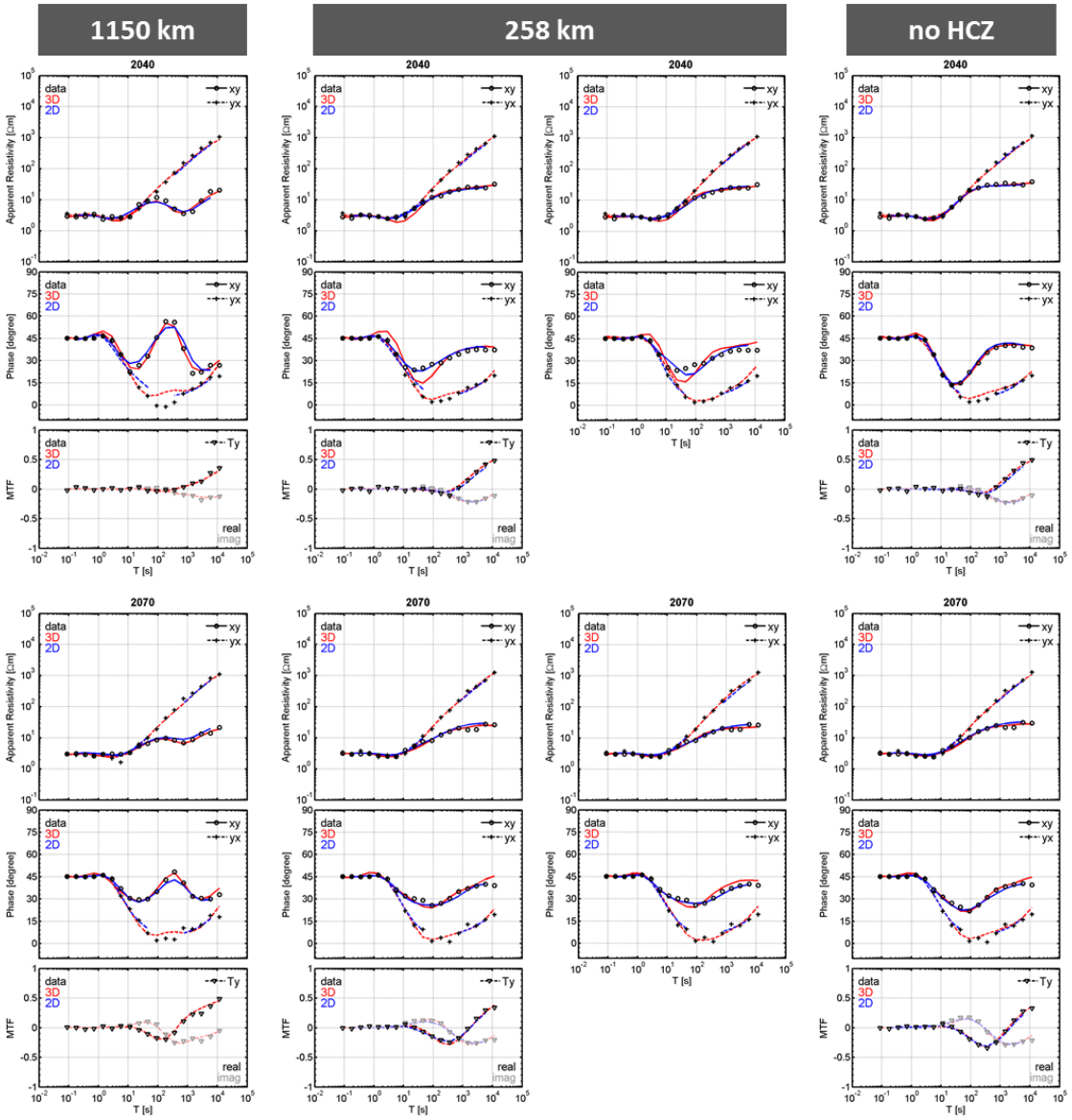

Figure 7: Comparison of 3D and 2D responses for joint (all) and impedance-only (258 km) inversion results. Site locations are marked in Figs 5 and 6. 3D and 2D data fits generally are of similar quality. For the shortest HCZ extent (258 km), 3D xy-phases between 1 s and 100 s systematically differ and indicate the absence of the HCZ in the inversion result. The blurred conductive region replacing the HCZ in 2D impedance-only result, however, does not have a significant effect on the data fit. Phase values below 5° had to be omitted in 2D inversion (see text).

The data fits of 3D and 2D inversion results are mostly of similar quality (Fig. 7). Where 3D inversion fails to recover the HCZ for the shortest along-strike extent of 258 km (middle column), 2D inversion responses better reflect the SYNPRK data. However, in order to successfully invert the data set in 2D, we had to exclude not only yx-phases below 0° but also those close to 0° which occur in the period range between 10 s and 200 s (gaps in 2D inversion responses). The 3D FWD responses contain phases which are very close to, but above 0°; phase values below 0° result from the Gaussian noise added to the impedance data prior to inversion. If yx-phases between 0° and 5° are not masked, 2D inversion fails to converge and introduces misleading artificial structures beneath affected sites (Fig. 8). We tested various modifications of the 2D resistivity structures, e.g. enhancing or decreasing resistivity contrasts between the Pacific Plate and the surrounding structures. It seems that there is a level of saturation for the 2D FWD modelling of high conductivity contrasts as we could not achieve yx-phase values below 3°.

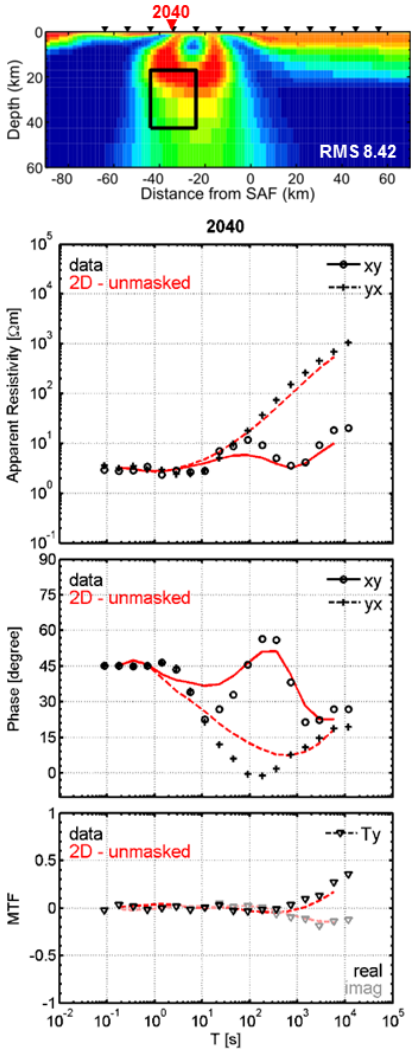

Figure 8: 2D inversion results of SYNPRK-1150 km. If yx-phase values close to or below zero are not masked, 2D inversion introduces artificial structures and fails to converge.

Discussion and conclusions

In most cases, both 3D and 2D inversion recovered the 3D HCZ successfully. The reliability of the subsurface structure depends on the inverted quantities. Best results were achieved for joint inversion of impedance-derived quantities and VTFs, particularly for 2D inversion. However, we encountered some unexpected obstacles for both inversion approaches.

For 3D inversion the largest challenges are the required wide range of resistivities and the strong conductivity contrasts of the SYNPRK model. The insufficient reproduction of extended zones of high resistivities beneath the ocean in the 3D inversion models impaired and partly inhibited resolution of the HCZ at depth.

2D inversion, using a different regularization scheme, detects even shorter versions of the structure. Inverting responses including a 3D ocean, the HCZ is systematically located at too shallow depth and artificial conductive structures appear. 2D inversion fails if phase values below 5° are not masked.

In conclusion, the advantages of joint inversion and both 3D and 2D modelling approaches should be used complementarily to render a comprehensive interpretation of the entire data set.

References

Becken, M., Ritter, O., Bedrosian, P. A. & Weckmann U., 2011. Correlation between deep fluids, tremor and creep along the central San Andreas fault, *Nature*, 480, 87—90.

Becken, M., Ritter, O., Park, S. K., Bedrosian, P. A., Weckmann, U. & Weber, M., 2008. A deep crustal fluid channel into the San Andreas Fault system near Parkfield, California, *Geophys. J. Int.*, 173, 718—732.

Caldwell, T. G., Bibby, H. M. & Brown, C., 2004. The magnetotelluric phase tensor, *Geophys. J. Int.*, 158, 457—469.

Egbert, G. D. & Kelbert, A., 2012. Computational Recipes for Electromagnetic Inverse Problems, *Geophys. J. Int.*, in press.

Ledo, J., 2005. 2-D versus 3-D Magnetotelluric data interpretation, *Surv Geophys*, 27, 111—148.

Mackie, R.L., Rodi, W. & Watts, M.D., 2001. 3-D magnetotelluric inversion for resource exploration, in *Proceedings of the 71st Annual International Meeting,* SEG, Expanded Abstracts, pp. 1501—1504.

Mackie, R. L., Smith, J. T. & Madden, T. R., 1994. Three-dimensional electromagnetic modeling using finite difference equations: The magnetotelluric example, *Radio Sci.,* 29, 923—935

Newman, G. A., Recher, S., Tezkan, B. & Neubauer, F. M., 2003. Case History: 3D inversion of a scalar radio Magnetotelluric field data set, *Geophysics*, 68, 791—802.

Rodi, W. & Mackie, R. L., 2001. Nonlinear conjugate gradients algorithm for 2-D magnetotelluric inversion, *Geophysics*, 66, 174—187.

Siripunvaraporn, W., Egbert, G., Lenbury, Y. & Uyeshima, M., 2005a. Three-dimensional magnetotelluric inversion: data-space method, *Phys. Earth Planet. Inter.*, 150, 3—14.

Siripunvaraporn, W., Egbert, G. & Uyeshima, M., 2005b. Interpretation of two-dimensional magnetotelluric profile data with three-dimensional inversion: synthetic examples, *Geophys. J. Int.*, 160**,** 804—814.

Tietze, K. & Ritter, O.. 3D magnetotelluric inversion in pratice, subm. to *Geophys. J. Int.*

Methods

3D modelling and inversion

The 3D model mesh consists of 50 × 70 × 57 cells in the two horizontal and the vertical directions, respectively, with the x-axis pointing towards N41°W. The central part of the mesh comprises 20 × 40 × 57 horizontally even-sized cells with an edge length of 4 km. On all four sides, the central domain is padded by 15 planes with cell sizes increasing laterally by a factor of 1.3. The vertical thickness is 25 m for the first layer and successively increases by a factor of 1.2 with depth. For the examples shown here, identical grids were used for FWD modelling and inversion.

2D modelling and inversion

The 2D inversion results shown here were achieved using a grid with approx. uniform horizontal spacing of 2 km. Smoothing parameter τ was set to 10 combined with horizontal (α=1.0) and vertical (β=1.5) weighting. 2D FWD modelling was conducted on the same grid as well as on a grid, which was refined in the vicinity of conductivity contrasts and sites.